Single Crystal High-Temperature Shape-Memory

Project WBS Number: 694478.02.93.11.14.22

Investigator(s): Glen Bigelow – GRC-RXA, Dr. Jon Goldsby – GRC-RXC
Dr. Anita Garg – University of Toledo, Dr. Ronald Noebe – GRC-RXA

Purpose

The objective of the Phase I was to first develop and then validate a new single crystal growth capability, specifically tailored for growing single crystals of shape memory alloys (SMAs), and then to develop and optimize single crystal SMAs with high temperature capability. This effort was not to replace our existing efforts on polycrystalline SMA development, but to leverage that knowledge by providing a method for producing materials with even greater shape memory and superelastic properties. Studies of single crystals are frequently used to explore fundamental materials behavior, but are also commercially relevant, as for example in the electronics industry as well as superalloy turbine blades.

Background

A major challenge in producing single crystal SMAs is that NiTi-based alloys are difficult to melt, primarily because the high Ti content in the alloys is very reactive with ceramic and graphite crucibles employed in conventional single crystal growth processes. A single crystal, which was previously studied, was grown in Russia by the Bridgman technique using a graphite crucible. Therefore, although it possessed exceptional properties, it also contained large carbides, which would diminish actuator performance and impact fracture and fatigue behavior. Due to this carbon contamination, the preferred solidification techniques should be restricted to containerless or cold-hearth processes such as were used in the Czochralski (CZ) single crystal growth furnace in the Ceramics Branch at NASA GRC. Using the Czochralski method, the SMA material was melted in a water-cooled copper crucible under a high purity argon atmosphere. The melting was achieved via arc melting with three tungsten electrodes, which allows for uniform heating and homogeneous melt composition during the process. The crystals were then produced by dipping the end of a tungsten or NiTiHf pull rod in the melt and withdrawing it at a controlled rate to allow a crystal to nucleate and grow from the melt. This method allowed us to grow high purity single crystals and thus avoid the detrimental effects of additional carbon and oxygen contamination. The knowledge and materials being developed in this Seedling Fund project will allow shape-memory alloys to be used in more demanding and varied applications, due to the improvements in work output available in the single crystal materials.

Approach

Crystals were produced using the tri-arc CZ furnace from Ni-Ti-Hf and Ni-Ti-Pd alloy compositions previously developed at GRC. This provided an opportunity to compare the properties of the grown crystals to our baseline polycrystalline material and with single crystals originally produced in Russia using the Bridgman technique. The first sets of CZ crystals grown were already much cleaner than the Bridgeman grown crystals, but contained tungsten particles from the arc melting process. We subsequently modified our arc melting procedure in order to produce even cleaner crystals without any tungsten particles. The single crystals were characterized via electron microscopy and other analytical techniques for determination of microstructure, purity and stress-free transformation temperatures and then tested mechanically for actuator performance. Thermomechanical testing via load-biased thermal cycling was used to measure dimensional stability, transformation strain, and work output under stress.

Summary of Research

Two of the high-temperature shape-memory alloys target compositions previously investigated in polycrystalline form at GRC are Ni-49.7Ti-30Pd and Ni-29.7Ti-20Hf (atomic %). Hot tops from vacuum induction melted and cast ingots of these compositions were used as precursor materials for growing single crystal samples via the Czochralski method so that the properties of the polycrystalline material and grown single crystals could be compared. Initially, a few different materials, namely alumina and thoriated tungsten were investigated as pull rods. The thermal conductivity of the alumina was too low to produce a good crystal, and only a small bulbous sample was grown (Figure 1a). The tungsten rods, however, produced longer samples, but because the rod diameter was ~4.8mm the samples grown were also small in diameter (Fig 1b). Therefore, larger 6.4mm diameter rods were machined and used to grow larger diameter samples (Figs 1c, 2). In all the samples produced, growth bands were visible, which are an indication of temperature and/or compositional inhomogeneity in the sample during growth. Arrows in Figure 1 and the line in Figure 3 (and region composed of martensite twins) indicate a few of these growth bands.

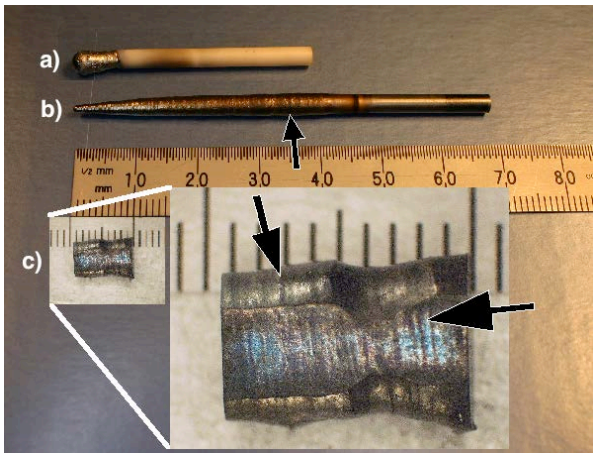

Figure 1. Some of the single crystal HTSMA samples grown: a) NiTiPd, b) NiTiPd, and c) section of NiTiHf.

Figure 2. Set of larger NiTiHf single crystals.

Figure 3. SEM image of NASA grown NiTiPd single crystal at 500x. 1)TiC 2)W (Line marks edge of band)

One sample of NiTiHf and one sample of NiTiPd was ground and polished along the length of the sample and then etched to reveal the microstructure. The samples were imaged using optical microscopy and SEM to determine the phases present and the presence of any grain boundaries. In the NiTiPd sample, TiC and W particles were present (Figure 3), while TiC/HfC and W particles were present in the NiTiHf sample (Figure 4).

The W particles are minimal, but are an effect of erosion of the W arc melting electrodes during melting as seen in Figure 5. The W rods are ground at a specific angle to a point and the tip flattened before use. As seen in Figure 5a, the

used electrode shows darkening around the tip due to the extremely high arc temperature, which leads to erosion of the W at the tip. This erosion of the tip can be seen more clearly in Figure 5b. We have been investigating methods to minimize W in the melt by using larger electrodes, different tip angles, and different W alloy electrodes with lower erosion characteristics. In doing this, we have produced several crystals with W levels low enough as to be unseen in the SEM and are only detectible through chemical analysis of the samples (Table 1)

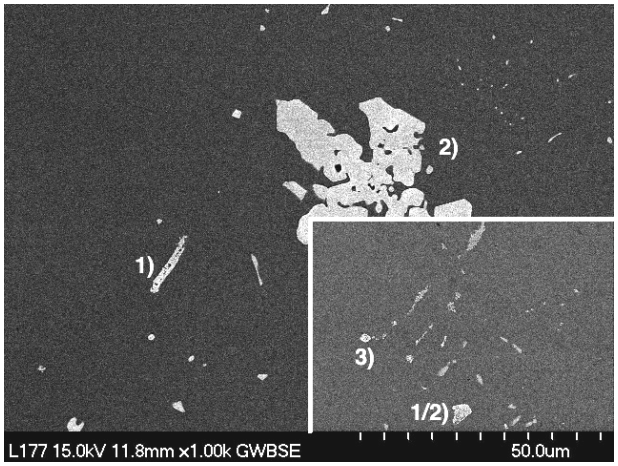

Figure 4. SEM image of Russian and NASA (inset) grown NiTiHf single crystal at 1000x. 1)HfO 2)HfC 3)W

The TiC/HfC particlesm, however, are a brittle unwanted second phase. While there are TiC/HfC particles in our materials, the carbon present is an inevitable result of the VIM melting method used to produce the initial ingot feedstock for the CZ process. This same carbon level was present in the feedstock for the Russian crystals, but it can be seen that the hafnium carbides present in the Russian crystals are up to an order of magnitude larger than the ones in our CZ produced samples due to the additional carbon introduced during the Bridgeman process. By melting in a cold hearth, we have avoided additional carbon, and thus have minimal TiC/HfC impurities. In Phase II we will investigate carbon free feedstocks to produce single crystals with minimal to no impurity phases.

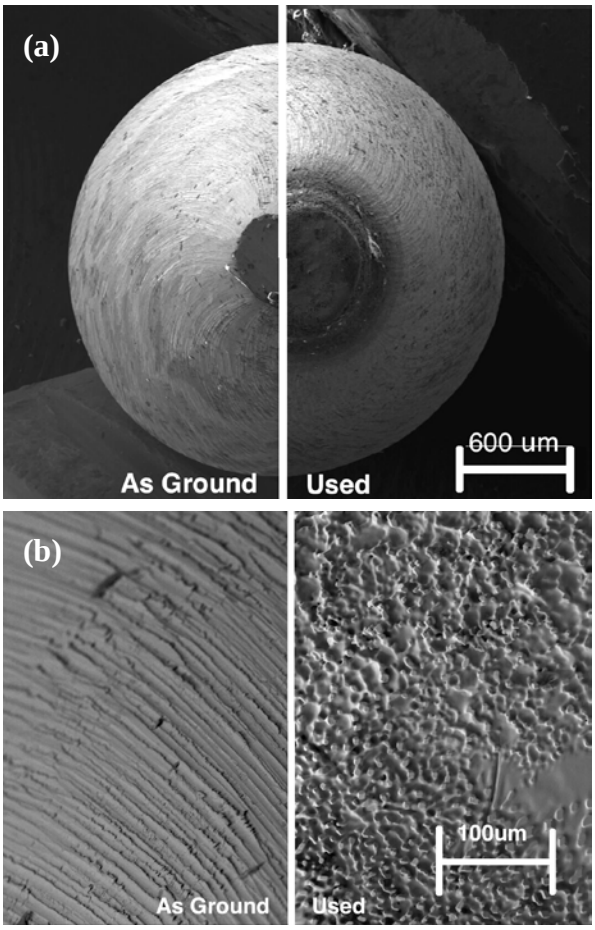

Figure 5. Low magnification (35X) (a) and higher magnification (250X) (b) images of the tungsten electrode tip in the as-ground and used conditions.

Although martensite twins are not always normally visible in optical and SEM images, the fact that they are visible in some regions while not in others in these crystals is another indication of chemical inhomogeneity. The lack of any visible grain boundaries is a good indicator that the grown samples are single crystals, as normal polycrystalline materials will have grain boundaries visible along the length of the sample. However, in directionally solidified polycrystals, the grain boundaries run

parallel to the growing direction, and would only be visible if the ground and polished portion coincided with the position of a grain boundary. Slices of the cross section were polished and etched but due to the martensite present at room temperature, did not definitively indicate or rule out grain boundaries.

The samples were then cut perpendicular to the growth direction via wire EDM to produce samples for chemical analysis, microscopy (optical, SEM and TEM), DSC, and X-ray. Chemical analysis samples of the 1st generation crystals were taken from both the top (next to the pull rod) and bottom of the samples, and the results of the analysis compared to the hot top precursors in Table 1. For the 1st gen NiTiHf sample (SX Hf148), no overall inhomogeneity or gradient is apparent and the material at both the top and bottom of the crystal is equivalent in composition to the hot top. The NiTiPd sample (SX Pd) from the top of the sample shows an extremely high amount of tungsten, which most likely is a result of part of the tungsten pull rod being cut off with the sample, skewing the measured composition of the other elements. The bottom sample has a composition equivalent to that of the precursor material. Once the homogeneity at the top and bottom of the crystal were assured, only one chemical analysis sample was taken, as is the case for the 2nd gen NiTiHf sample (SX Hf149) which shows a composition equivalent to that of the precursor hot top. In addition, due to the improved melting practices, the W in the sample has been nearly eliminated, at only 0.02%, compared to the 1st gen alloys at 0.15 and 0.28% W.

Table 1: Chemical Analysis of HTSMA Single Crystal Samples and Precursor Hot Top Material.

Sample	Ni	Ti	Hf	Zr	Pd	W
HT148	50.5	29	20.0	0.4		
SX Hf148 T	50.2	29	20.4	0.3		0.15
SX Hf148 B	50.2	29	20.3	0.31		0.16
HT149	50.1	29.8	19.9	0.3		
SX Hf149	50.5	29.7	19.5	0.3		0.02
HT160	20	48.9			31.1	
SX Pd160 T	16.1	43.7		0.03	26.8	13.4
SX Pd160 B	19	48.9		0.04	31.8	0.28

Transformation temperatures from both the top and bottom of each sample were measured using DSC, and the data compared to as received and heat-treated polycrystalline material of the same compositions in Figure 6. Although the chemical analysis of the NiTiHf alloy didn't reveal any overall inhomogeneity in the sample, the DSC data in Figure 6a clearly shows that very different transformation temperatures occur in the top (-1M_F 127A_F) and bottom (-22M_F 99A_F) of the sample. In addition, the transformation peaks are extremely broad compared to the polycrystalline material and are a superposition of many different transformation peaks. This again is likely the result of the inhomogeneity in the growth bands creating regions with widely varying transformation temperatures. The top (72M_F 144A_F) and bottom (85M_F 146A_F) of the NiTiPd sample show transformations that are much narrower than those of the NiTiHf samples (Figure 6b), but are still broad compared to the polycrystalline material, again, most likely due to inhomogeneity. However, the transformation temperatures are close to those of the as received polycrystalline material.

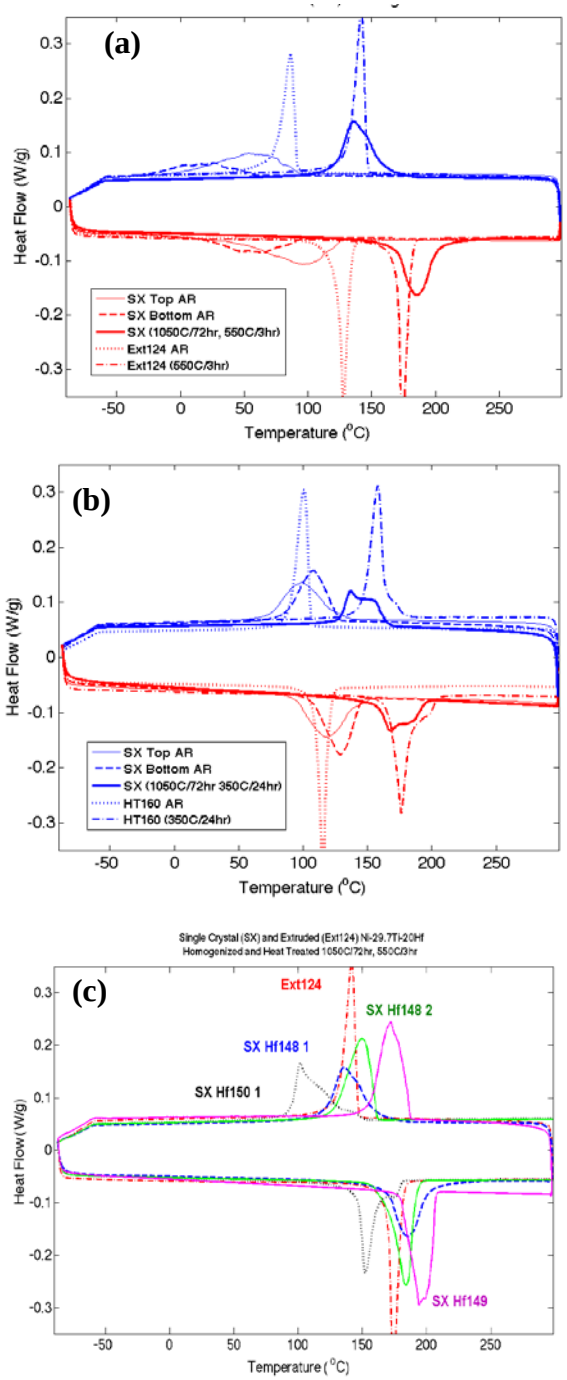

Figure 6. a) Single crystal (SX) and extruded (Ext124) as received (AR) and aged Ni-29.7Ti-20Hf, b) Single crystal (SX) and hot top (HT158) as received (AR) and aged Ni-49.7Ti-30Pd, and c) Single crystal 1st, 2nd, and 3rd gen NiTiHf samples compared to polycrystalline material (E124)

Because of the issues with inhomogeneity and the low transformation temperatures of the as-grown samples, the remainder of the material from each sample was heat-treated using the heat treatments developed for the polycrystalline materials. Both samples were homogenized at 1050ºC for 72hrs and then aged at 550ºC for 3 hrs for the NiTiHf and at 350ºC for 24 hrs for the NiTiPd. Specimens for DSC, microscopy, X-ray, and mechanical testing were cut from the heat-treated samples. DSC testing of the heat treated samples shows that the transformation temperatures have been increased and the peaks narrowed due to the heat treatment and are equivalent to those of the heat treated polycrystalline material in both the NiTiHf and NiTiPd samples. This shows that inhomogeneity in the samples can be solved via heat treat and will not be an issue. Although 1st, 2nd, and 3rd gen single crystal materials were produced from three different precursor ingots, which have chemical variations between them, the single crystals from HT148 have final transformation temperatures similar to each other and the other single crystals only vary from that by ~50ºC.

In addition, cross-sectioned samples of the as grown material were prepared for microstructural analysis and X-ray analysis. When the material is in the low temperature martensite phase, many different twin variants are present in the crystal, which in x-ray, scatter the waves, similar to a polycrystalline material. Therefore, a heating fixture was built which allows for X-ray analysis of the materials at high temperature in the austenite (where twin variants are not present) to better determine if the materials are truly single crystalline, and their orientation. Figure 7 shows the XRD results of the NiTiHf single crystal (Run#2 from HT148). The data was gathered from a cross-sectioned surface of the sample using a Bruker D8 Diffractometer with a General Area Diffraction Detector System (GADDS) area detector and a Material Research Inc. (MRI) BTS-Solid heating stage. Cu Kα radiation was used with a 0.5mm diameter collimator. The

figure shows only the central portion of the pole figure where data was gathered, and the stereographic net is shown in 10° increments. The boxed yellow region indicated the data coverage, and the red spots represent individual crystal grains. About 13 grains can be seen in the pole figure with an orientation spread of 15° - 20°. The mean region covered by the x-ray beam was about 0.5μm^2 (elliptical pattern on surface). Assuming that all grains present in the beam region were captured, this data implies a typical grain diameter in the plane of the cross-section of about 220μm.

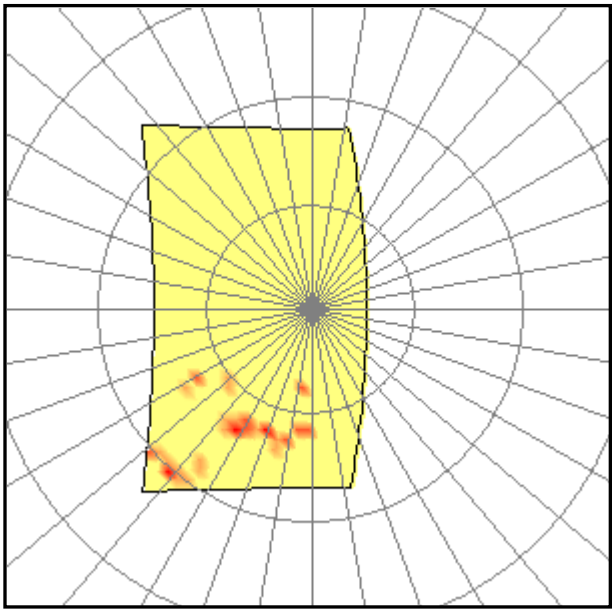

Figure 7. Partial pole figure of the (200) pole of the aged NiTiHf SX (Run#2) in the austenite phase at 200ºC in air.

Thermomechanical load-biased testing of the Ni-29.7Ti-20Hf crystal was performed in compression in steps up to -1500MPa, wherein the sample was loaded in martensite to the desired stress, held in force control and thermally cycled twice before loading to the next stress level. From this test, the transformation strain, work output and dimensional stability of the sample were determined (Figure 8 (a,b,c)) and show that the CZ grown single crystal (SX2) has properties approximately equivalent to, or better than those of the Russian grown single crystals (SX). These plots show that the commercial binary 55NiTi alloy, which has the highest available transformation temperature exhibits transformation strains as high as 3.5%, but this occurs at relatively low stress (300MPa), and then declines at higher stress levels (Figure 8a). For polycrystalline NiTiHf (Ext 124), the maximum strain of 2.2% occurs at much higher stress (700MPa). Depending on orientation, a single crystal of the same NiTiHf composition can exhibit either higher strain (3.4%) at the same stress for the [-340], or moderate strain (0.6-0.75%) at extremely high stress levels for the [001], which is a great improvement over the polycrystalline material. Even though the 55NiTi alloy has higher transformation strain than the NiTiHf materials, because work output is a product of the applied stress and transformation strain, the work output of the polycrystalline and single crystal NiTiHf materials is at least equivalent to that of 55NiTi, and in some orientations is more than double. In addition, because the work output of the single crystals comes at much higher stress levels, a smaller amount of the HTSMA is needed, which means that these single crystal materials can be used in more compact and much more demanding actuators. Figure 8c shows that the dimensional stability (the ability of an actuator to repeatably return to the same position during cycling) of the NiTiHf polycrystalline and single crystals is nearly perfect up to stresses of 700MPa (polycrystalline, [678], and [-340]) and 1100MPa ([001]). Also the dimensional stability of the GRC CZ grown material is nearly identical to the [001] up to 1100MPa and only deviates slightly after that. Thus, it appears that the GRC CZ grown NiTiHf crystal is [001] orientation or near it.

The mechanical test data from the CZ grown NiTiPd sample is shown in Figure 9 (a,b,c). Although the transformation strain in the SX sample is not as high as that of the polycrystalline material, the stress capability of the sample is 100 to 200MPa higher. The work output, while lower than that of the polycrystalline material, is stable out to at least 1000MPa. The dimensional stability of the material is better than that of the polycrystalline material by a factor of 2.

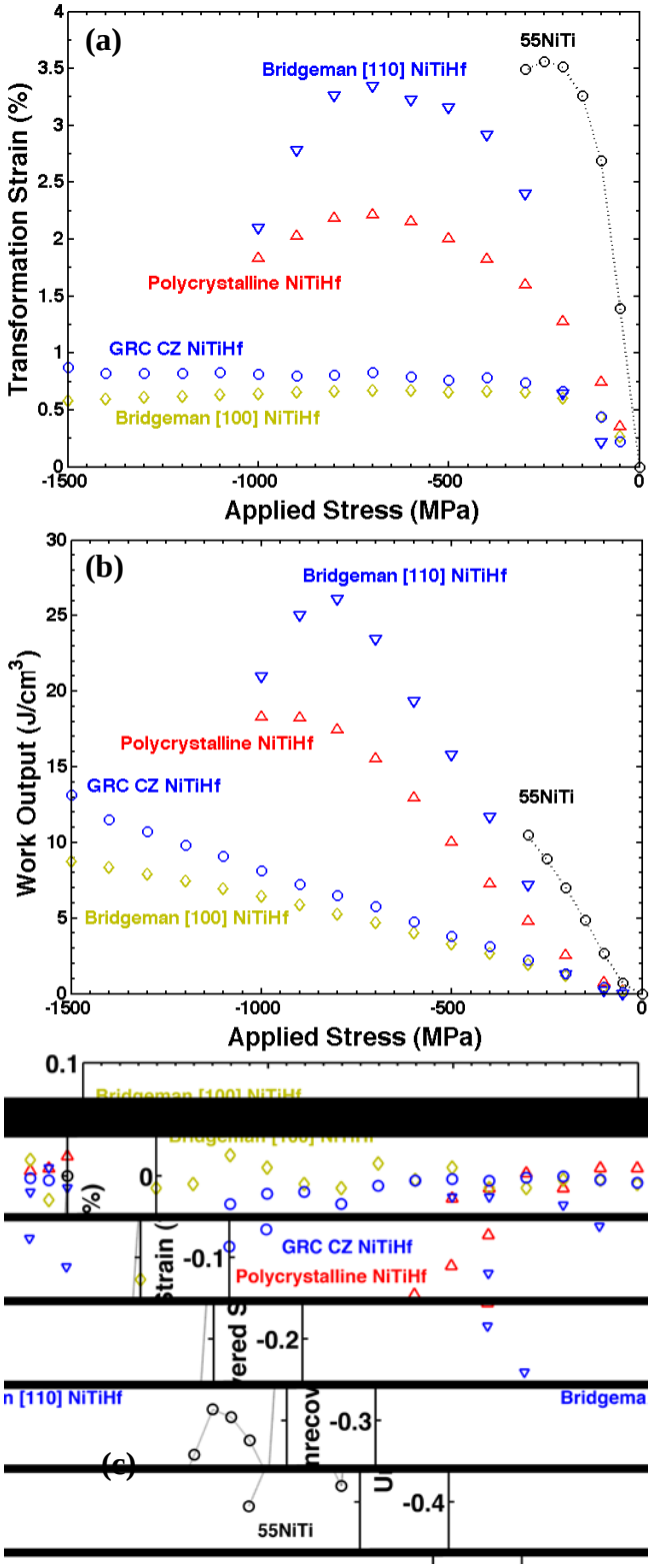

Figure 8.a) Transformation strain, b)Work, c)Unrecovered strain for polycrystalline NiTi (55NiTi) and NiTiHf, Bridgeman grown single crystals, and GRC CZ grown single-crystals.

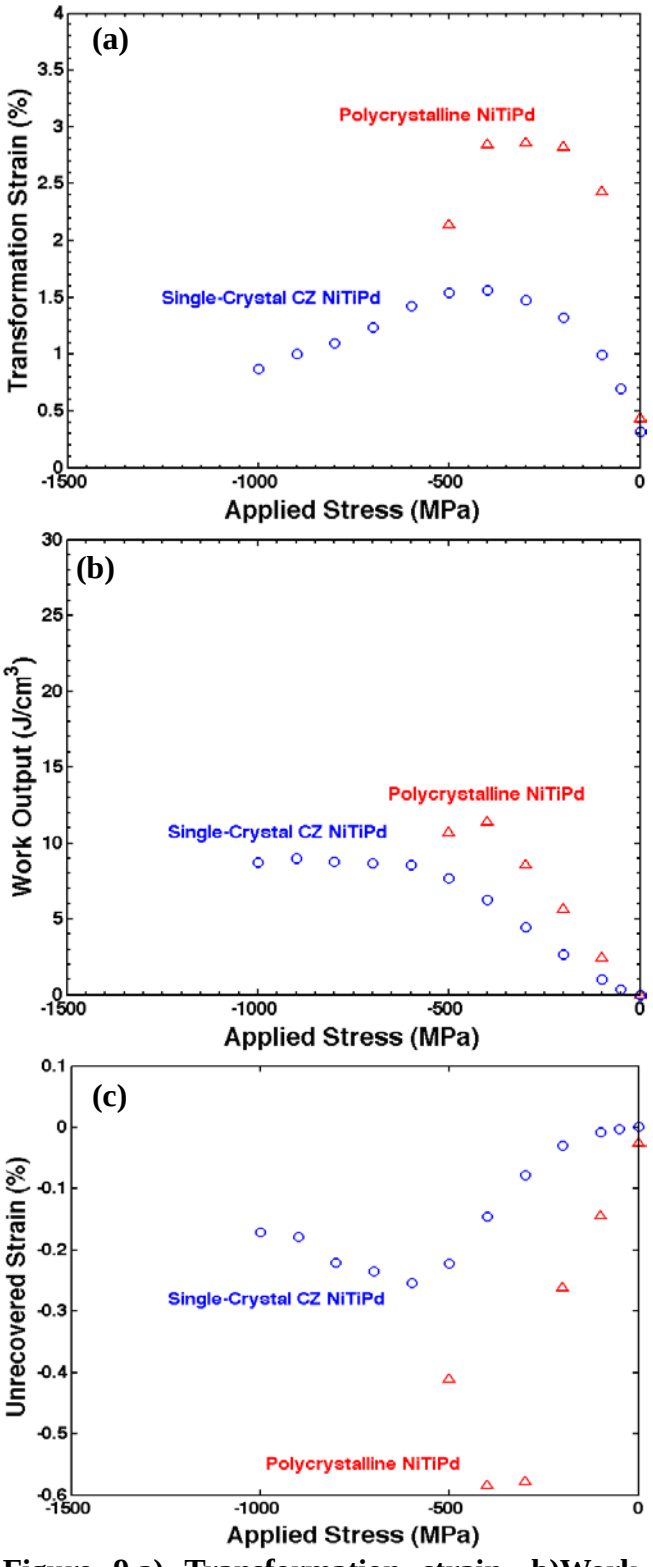

Figure 9.a) Transformation strain, b)Work, c)Unrecovered strain for polycrystalline NiTiPd and GRC CZ grown single-crystals.

In addition, samples of the second iteration of Ni-29.7Ti-20Hf single crystals have been homogenized and heat treated and will be tested in the following weeks.

Milestone	Completion Date	Status
1) Rehab of CZ growth furnace	7/11	
2, 4) Growth of 1st and 2nd iteration of NiTiHf	7/11, 3/12	Ni-Ti-Pd and Ni-Ti-Zr crystals additionally grown.
3) Microstructural and mechanical characterization of 1st gen. crystals	5/12 – Ni-Ti-Hf 6/12 – Ni-Ti-Pd	
5) Microstructural and mechanical characterization of 2nd gen. crystals	8/12 – Micro & Chem	Mechanical testing underway – to be included in TM
6) Growth of higher temperature SMA	5/12 – Ni-Ti-20Hf	Additional Ni-Ti-20Hf samples produced instead.
7) Microstructural and mechanical characterization of 25Hf crystals.	8/12 – Micro & Chem	Mechanical testing underway – to be included in TM

Accomplishments

The Czochralski single crystal growth furnace was modified for growing single crystal SMAs. In addition to the Phase I proposal promise of producing two iterations of Ni-29.7Ti-20Hf single crystals using the Czochralski method, we have also produced single crystals of two other alloys, Ni-49.7Ti-30Pd, and Ni-29.7Ti-20Zr (at.%). Microstructural, chemical, and thermal analysis of the as-grown Ni-Ti-Hf and Ni-Ti-Pd samples has been performed. Inhomogeneities in samples have been overcome via homogenization and heat treatments. Mechanical testing of NiTiHf samples has been completed, which shows properties equivalent to those produced by Russian grown single crystals of the [001] orientation. A heater setup has been built and tested and is in use to allow high-temperature x-ray analysis of the materials. The available data thus far indicates that the samples are single crystal, and x-ray analysis is underway to confirm this and determine the orientation of the grown crystal. Mechanical testing of the tungsten free Ni-29.7Ti-20Hf alloy is scheduled.

Next Steps

A Seedling Fund Phase II award has been granted for this project. In the Phase II effort, large diameter and small diameter crystals will be produced to study the effect of size on the crystal properties. With successful completion of the Phase II effort, the single crystal project will most likely be phased into either Subsonics Fixed Wing or Aero Sciences as an extension of the polycrystalline SMA work already being done.

Current TRL: 2

Applicable NASA Programs/Projects

Shape memory alloys (SMAs) are being actively pursued by tasks in SFW and Supersonic projects in the Fundamental Aeronautics Program. Much of our in-house efforts in these two projects have been focused on developing new polycrystalline alloys with improved temperature and stress capability compared to commercially available NiTi SMAs, expanding the range of applications where these materials can be used, including both airframe and engines. Additionally, modeling tools are being developed for use of such alloys to reduce training time and enable 3-D actuation. There are no research activities in SFW and Supersonic projects to develop single crystal shape memory alloys. This will not replace our existing efforts on polycrystalline SMA development, but will leverage that knowledge by providing a method for producing materials with even greater shape memory and superelastic properties. The scientific knowledge gained from single crystal SMAs can be applied to improve the alloys and modeling tools being developed in SFW and supersonics projects.

Publications and Patent Applications

This Seedling Fund final report will be published as a NASA TM with an expanded section on mechanical testing, including the completed tests from milestones 5 and 6.

Awards & Honors related to Seedling Research

The Single Crystal High-Temperature Shape-Memory Alloy project was granted a Seedling Fund Phase II award.